

# Triana Safehold: A New Gyroless, Sun-Pointing Attitude Controller

J. (Roger) Chen (K&D Research), Wendy Morgenstern (GSFC), Joseph Garrick (GSFC)

## ABSTRACT

Triana is a single-string spacecraft to be placed in a halo orbit about the sun-earth L1 Lagrangian point. The Attitude Control Subsystem (ACS) hardware includes four reaction wheels, ten thrusters, six coarse sun sensors, a star tracker and a three-axis Inertial Measuring Unit (IMU). The ACS Safehold design features a gyroless sun-pointing control scheme using only sun sensors and wheels. With this minimum hardware approach, Safehold increases mission reliability in the event of a gyroscope anomaly. In place of the gyroscope rate measurements, Triana Safehold uses wheel tachometers to help provide a scaled estimation of the spacecraft body rate about the sun vector. Since Triana nominally performs momentum management every three months, its accumulated system momentum can reach a significant fraction of the wheel capacity. It is therefore a requirement for Safehold to maintain a sun-pointing attitude even when the spacecraft system momentum is reasonably large.

The tachometer sun-line rate estimation enables the controller to bring the spacecraft close to its desired sun-pointing attitude even with reasonably high system momentum and wheel drags. This paper presents the design rationale behind this gyroless controller, stability analysis, and some time-domain simulation results showing performances with various initial conditions. Finally, suggestions for future improvements are briefly discussed.

## INTRODUCTION

Triana is a mission dedicated to helping scientists construct more accurate models of the Earth's climate and to examining how solar radiation affects our climate. Triana is a single-string spacecraft destined for a Lissajous orbit about the Lagrangian point between the Earth and the Sun. This unique vantage point will provide Triana with a constant, sunlight view of the Earth.

Triana's on-board ACS software includes five different control modes: Science, Delta-V, Delta-H, Sun Acquisition and Safehold. During Science observations, the Triana ACS provides three axis stabilization with an accuracy of several arcminutes. Delta-V modifies the orbit trajectory, and Delta-H manages the spacecraft momentum. Sun Acquisition establishes a sun-pointing attitude. Safehold also establishes a thermal and power safe attitude, but it does so using a minimum hardware complement. This paper will focus on the design, implementation, and performance of Triana's gyroless Safehold control algorithm.

The Triana spacecraft, shown in Figure 1, uses a variety of sensors and actuators. Most of the hardware connects directly to the 1553 databus. A Honeywell Ring Laser Gyroscope (RLG) IMU provides rate information in all three axes. The star tracker is a Ball CT-633, which outputs an attitude quaternion. Triana includes two types of sun sensors. Six Adcole Coarse Sun Sensors (CSS) are arranged into three opposing pairs along three orthogonal axes for full sky coverage. Also on-board is an Adcole Digital Sun Sensor (DSS), which provides partial sky coverage with a  $\pm 64$  degree field of view and its boresight aligned along the sun-side solar array normal. The CSS and DSS are connected to the 1553 database through an interface known as the Utility Hub. Control actuation is provided by either reaction wheels or thrusters. Ten Kaiser-Marquardt one pound thrusters are arranged to provide both pure torque couples for attitude control and pure forces for changes in the orbit velocity. The thrusters are controlled by an Engine Valve Driver (EVD) card, which is also connected to the spacecraft databus via the Utility Hub. Four Integrated Reaction Wheel Assemblies (IRWA) are arranged in a

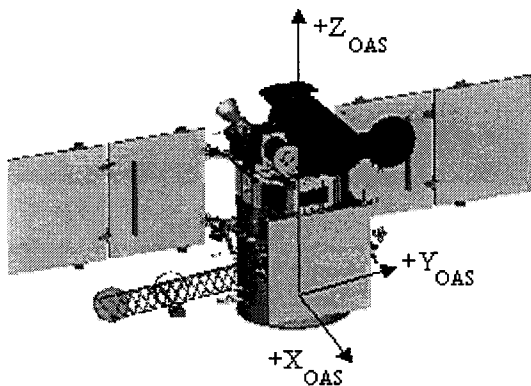


Figure 1: Fully Deployed Triana Spacecraft

pyramid configuration with the pyramid axis along the solar array normal.

Triana Safehold is a thermal and power safe sun pointing mode, based on a Proportional-Derivative (PD) controller providing commands to the IRWAs, similar to the Safehold mode for the MAP spacecraft.<sup>1</sup> What makes the Triana Safehold unique is its derivation of rate information. Since Triana does not carry redundant gyros, it is desirable to

have a Safehold mode, capable of safing the spacecraft in the event of a gyro anomaly. CSS data provides the attitude errors for Safehold and, through their differentiation, body rates for the axes perpendicular to the sun-line. However, the rate about the sun-line is unobservable with the CSS. Instead, the wheel tach information is used to derive a rate about the commanded sun-line.

## CONTROL LAWS

### Two-Axis Control

A control law for commanding three or four wheels with only 2-axis attitude knowledge afforded by the sun sensors plays the primary role in Triana's Safehold control. This control law is

$$\mathbf{T}_c = \mathbf{I} \{ \mathbf{k}_p \text{Limit}(\theta_e) + \mathbf{k}_v [(\frac{d}{dt}\mathbf{s}) \times \mathbf{s}] \}$$

$$\theta_e = \mathbf{s} \times \mathbf{s}_d$$

$$\mathbf{T}_{wc} = \mathbf{W}^+ \mathbf{T}_c + \mathbf{T}_{mr} + \mathbf{T}_{dc}$$

where the variables are

- $\mathbf{T}_c$  : commanded net wheel torque vector
- $\mathbf{T}_{wc}$  : column matrix (n by 1) consisting of individual wheel torque commands and n is the total number of wheels under control
- $\mathbf{I}$  : spacecraft inertia matrix (3 by 3)
- $\mathbf{s}$  : unit sun vector
- $\mathbf{s}_d$  : desired unit sun vector (nominally along body -X axis for Triana)
- $\mathbf{k}_p, \mathbf{k}_v$  : diagonal gain matrices (3 by 3)
- $\mathbf{T}_{mr}, \mathbf{T}_{dc}$  : column matrices (n by 1) consisting of wheel momentum redistribution and drag compensation torque commands for individual wheels
- $\mathbf{W}^+$  : pseudo-inverse (n by 3) of the wheel mounting matrix (3 by n), each column of which comprises the unit vectors along the positive spin axis of a wheel

Here and throughout this paper, a vector variable generally refers to a 3 by 1 matrix representation of a "basis-independent vector" in the unit vector basis fixed in the spacecraft's main body. Occasionally, a vector in a term will refer to a "basis-independent vector" itself and the term will be enclosed in quotation marks in this situation.

The "Limit" function in the above control law limits the absolute value of each element of the error angle vector  $\theta_e$  to some predefined parameter value and preserves its sign. The error rate vector, being the cross product of the time derivative of  $\mathbf{s}$  and  $\mathbf{s}$ , is approximately equal to  $\omega$ , the angular velocity vector of the spacecraft in inertial frame, without the component in the direction of  $\mathbf{s}$ . This is the case because the unit "sun vector" is changing its direction very slowly in an inertial frame and therefore the derivative of  $\mathbf{s}$  is approximately equal to  $-\omega \times \mathbf{s}$ . In this control law, momentum redistribution torque command matrix is used to minimize the maximum value of individual wheel momenta. Wheel drag compensation torque command matrix is meant to cancel a portion of the anticipated drag torque of each wheel so that the actual torque applied to each wheel is closer to what is commanded.

With this 2-axis control, a desired axis fixed in the spacecraft body represented by  $\mathbf{s}_d$  can be reoriented toward the sun from any arbitrary starting orientation. In ideal conditions this control law will align  $\mathbf{s}$  with  $\mathbf{s}_d$  in the steady state. The ideal conditions are those in which either the wheel drag torque is zero, which is physically impossible, or the wheel drag is exactly compensated. Figure 2 shows some response curves of the sun angle for Triana under the 2-axis control in the ideal condition. Here and throughout this paper, sun angle refers to the angle between  $\mathbf{s}_d$  and  $\mathbf{s}$ . Achieving a small steady-state sun angle from arbitrary initial orientation is thus the objective of a Safehold control. For Triana, the Safehold controller must reduce the sun angle to 15 degrees within 15 minutes. The sample responses seem to indicate the efficacy of the 2-axis control in achieving the desired goal of Safehold.

Results displayed in this section are all generated using a low-fidelity simulation with the control interval of 0.1 seconds and 1 cycle of computation delay consistent with Triana ACS implementation.

Even though this 2-axis control computes a 3-axis wheel torque command in each control cycle, only 2-axis measurements of the unit sun vector provide the feedback. Without the measurement in either angle or rate about the

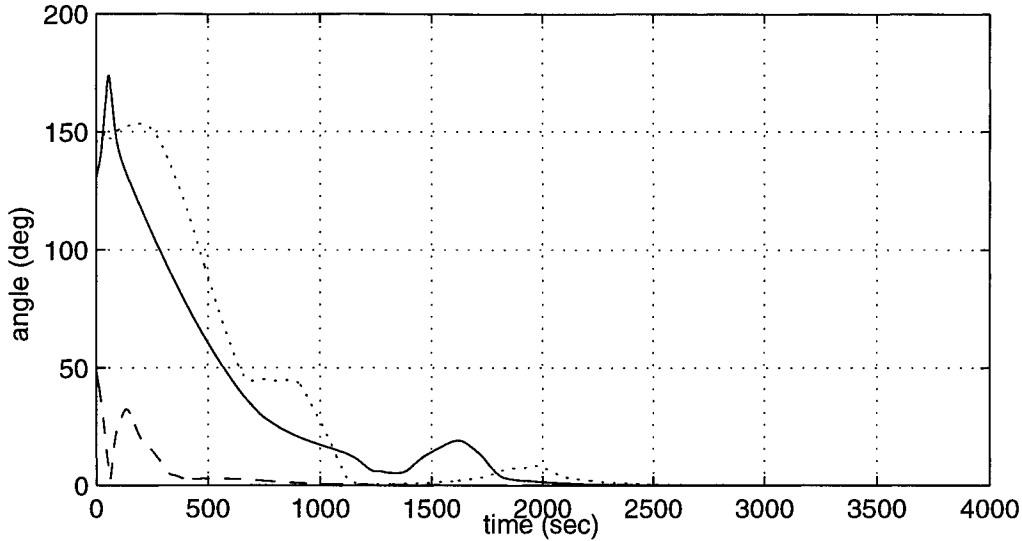


**Figure 2: Sample Sun Angle Results Due to 2-Axis Control in Ideal Conditions**

sun line, the system is not completely observable. This lack of feedback for one axis results in degraded sun pointing performance when the uncompensated wheel drag is included in the simulation. Figure 3 displays the simulation results of a case identical to the case yielding the solid line curve in Figure 2 except that the uncompensated wheel drags have some realistic non-zero values.

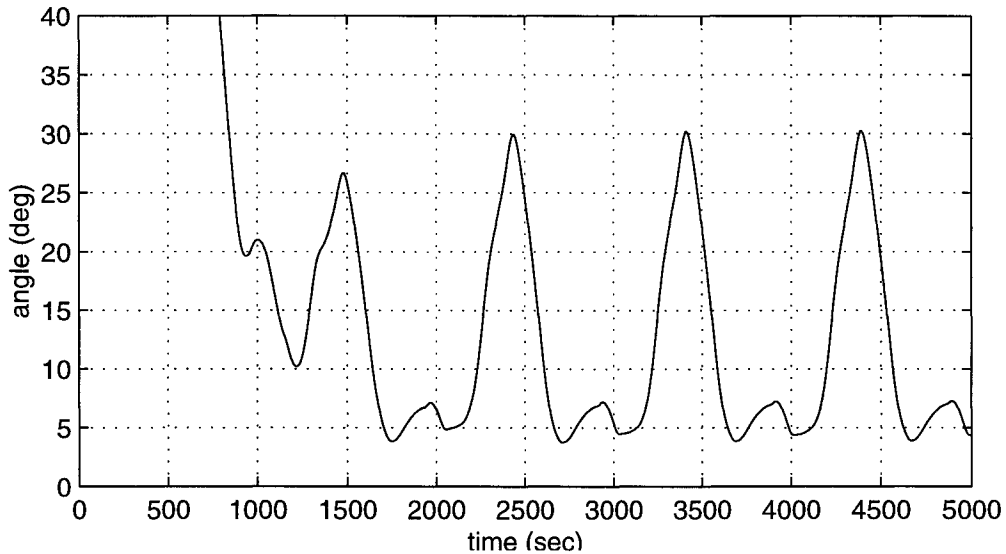


**Figure 3: Sun Angle For Triana under 2-Axis Control in Non-ideal Condition**

Not only does the steady-state sun angle deteriorate to a level beyond the 15 degree requirement, but also the wheel momenta and the wheel torque commands in Figures 4 and 5, respectively, show significant wheel activities in steady state. For Triana, reasonably high system momentum can occur due to the desire that the frequency of interruption caused by momentum management operations is minimized. Here system momentum refers to the magnitude of the system momentum vector, which is the sum of all inertial angular momentum of the spacecraft system with respect to the overall center of mass. Both high system momentum and uncompensated wheel drags can cause performance degradation; the greater their values are the worse the steady-state sun angle becomes. It is therefore desirable to have some enhancement of this 2-axis control that can provide improved steady-state sun angle performance.

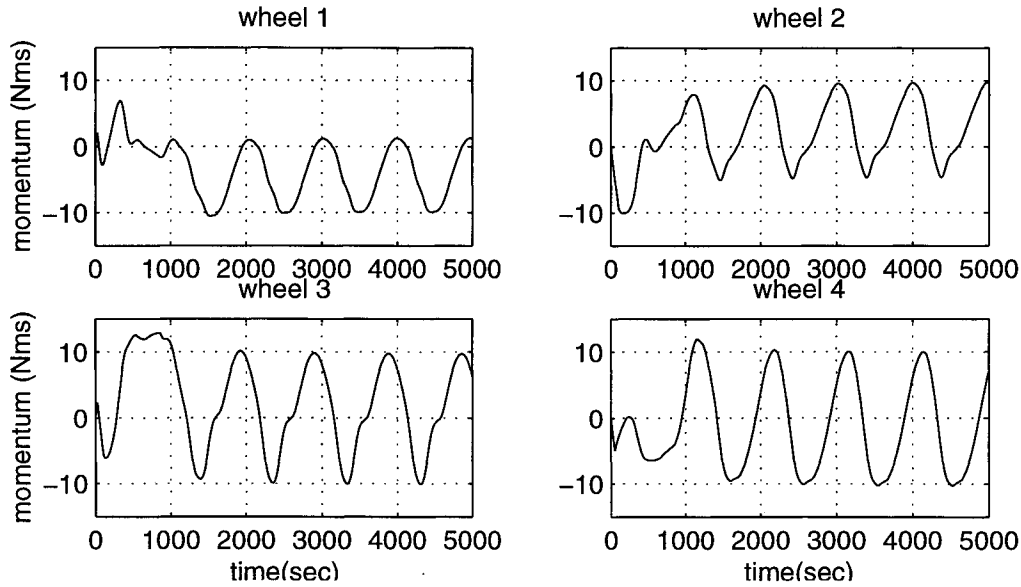


**Figure 4: Wheel Momenta for Triana under 2-Axis control in Non-ideal Conditions**

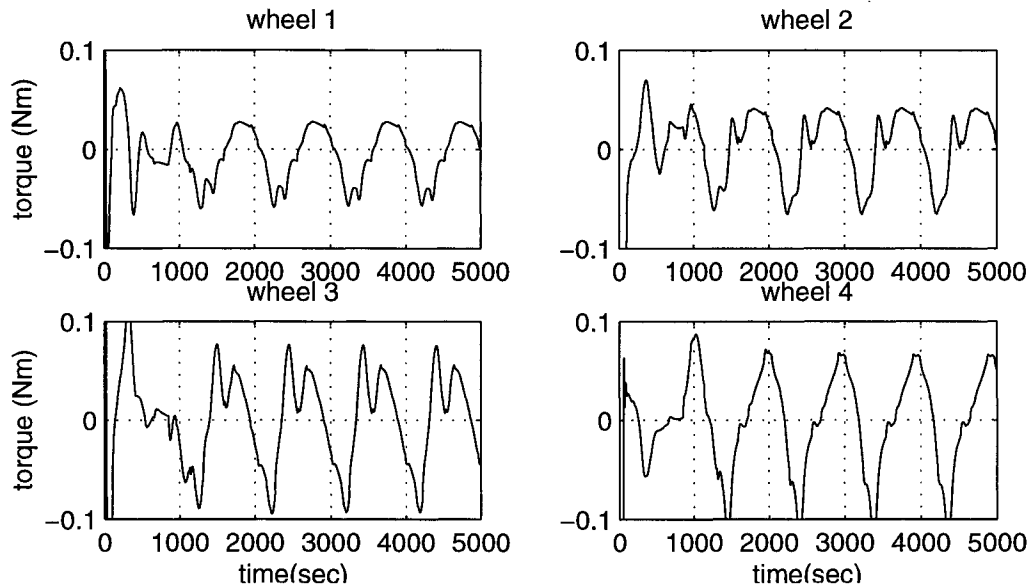
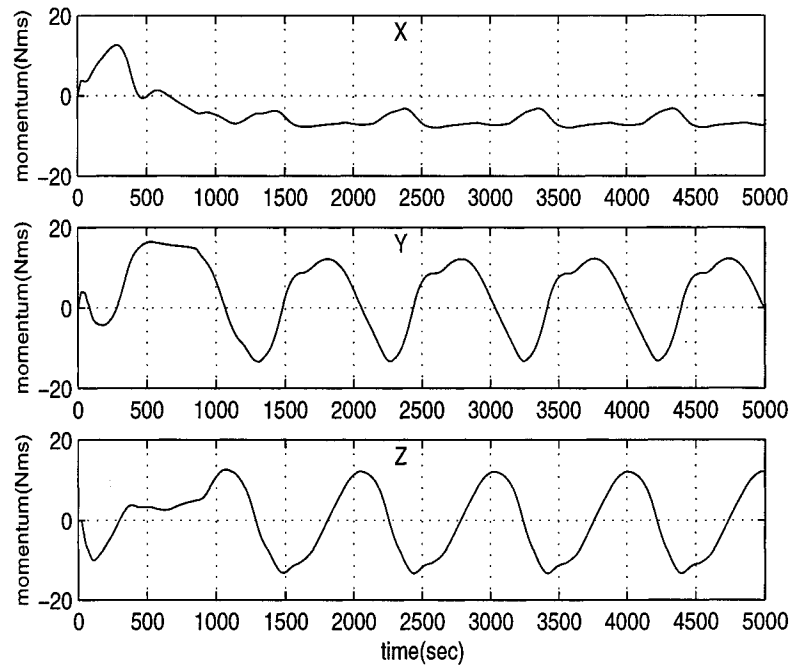


**Figure 5: Wheel Torque Commands For Triana under 2-Axis Control in Non-ideal Conditions**

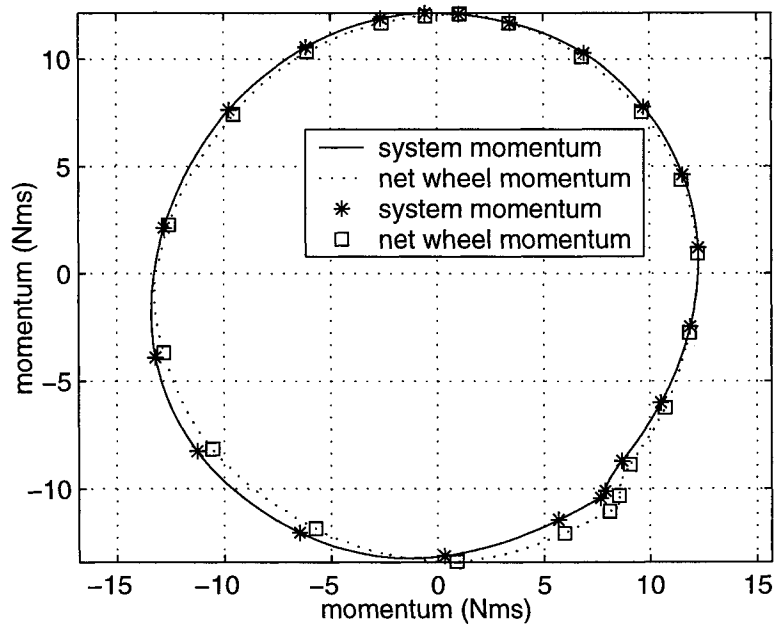
### Sun-Line Rate

Figure 4 shows that momenta of all four wheels in steady state exhibit slightly distorted sinusoidal fluctuations with the same frequency. These fluctuations imply that the net wheel momentum vector  $\mathbf{h}$ , which is the sum of the angular momentum vectors of individual wheels relative to the spacecraft body, should also show similar distorted sinusoidal fluctuations. In fact,  $h_y$  and  $h_z$ , the Y and Z elements of  $\mathbf{h}$ , respectively, also exhibit fluctuations with the same frequencies as can be seen in Figure 6. Notice that the desired sun line for Triana is the  $-X$  axis and thus the Y and Z axes are normal to the desired sun line. Since these two near sinusoids display roughly constant phase relations and similar magnitude, the curve obtained when one is plotted against another should be a distorted circle. Shown in Figure 7 are two traces:  $h_z$  vs.  $h_y$  and  $H_z$  vs.  $H_y$ , where  $H_y$  and  $H_z$  are, respectively, the Y and Z elements of

$\mathbf{H}$ , the 3 by 1 system momentum vector. Also shown on the two traces are markers corresponding to equally separated time points for the two traces. It can easily be observed from the markers that the component in YZ plane of  $\mathbf{h}$  is tracking closely that of  $\mathbf{H}$  in steady state. Notice that these traces repeat as time goes on in steady state; traces of any two dynamic variables when plotted one against the other will also repeat. This steady-state behavior is referred to as a periodic orbit in state space.<sup>2</sup>



**Figure 6: Net Wheel Momentum Vector Measurements under 2-Axis Control in Non-ideal Conditions**



**Figure 7: Z vs. Y Momentum under 2-Axis Control in Non-ideal Conditions**

This tracking of momentum vector components in steady state can be explained with the use of the system momentum equation,  $\mathbf{I}\omega + \mathbf{h} = \mathbf{H}$ . Since external disturbance torque for Triana is very small, the “system momentum vector” can be considered as fixed in an inertial frame for the duration of interest. Because of this, the short term variations of  $\mathbf{H}$  are entirely due to  $\omega$ . If the spacecraft experiences a pure X rotation, then the graph of Z vs. Y elements of  $\mathbf{H}$  will become a pure circle. For such pure X rotation to continue indefinitely, the Y and Z elements of the left hand side must be exactly equal to those of  $\mathbf{H}$ . If  $\omega$  is also constant then  $h_y$  and  $h_z$  must track  $H_y$  and  $H_z$  with perhaps a constant offset that is contributed by  $\mathbf{I}\omega$ . The steady-state motion of the spacecraft under 2-axis control is not a pure constant speed X rotation, but is not too far from it either as can be seen in Figure 8.

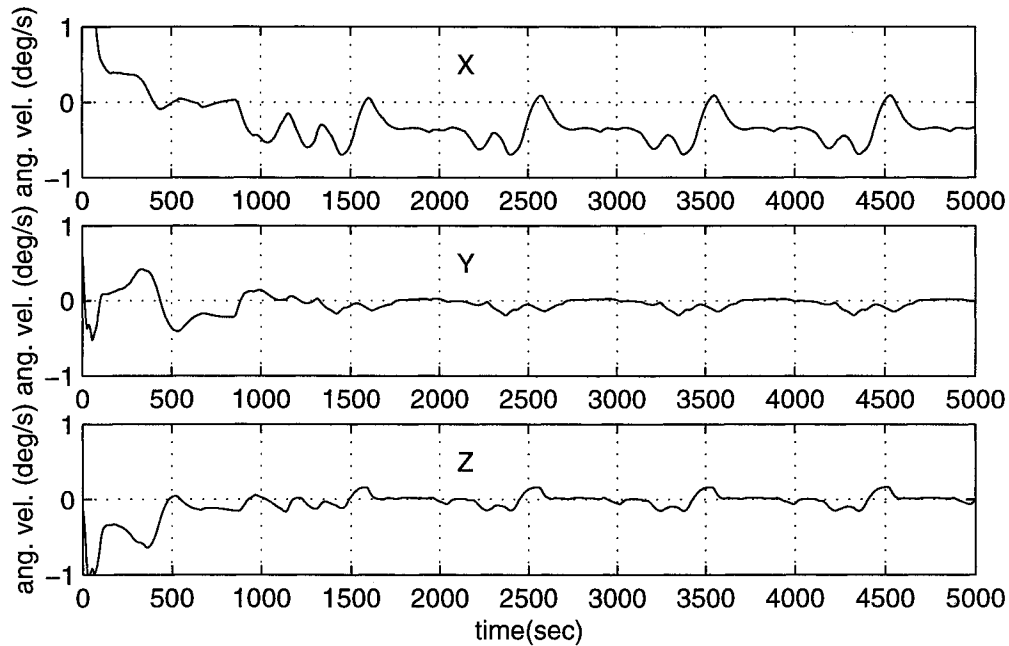


**Figure 8: Spacecraft Angular Velocity Measurements under 2-Axis Control in Non-ideal Conditions**

If, on the other hand,  $h_y$  and  $h_z$  do not track  $H_y$  and  $H_z$  sufficiently closely, their differences have to be absorbed by  $\mathbf{I}\omega$  and thus cause change in  $\omega$ , especially  $\omega_y$  and  $\omega_z$ , the Y and Z elements of  $\omega$ , respectively. Non-zero  $\omega_y$  and  $\omega_z$  implies that the spacecraft -X axis moves relative to the sun vector or the sun angle fluctuates; the greater  $\omega_y$  and  $\omega_z$  are, the greater the sun angle fluctuates. It can thus be argued that the 2-axis control law keeps the component of  $\mathbf{h}$  in YZ plane tracking that of  $\mathbf{H}$  closely in steady state so that the sun angle remains relatively small.

Since the steady-state attitude motion of the spacecraft under the 2-axis control is roughly an X axis rotation, the component of  $\mathbf{H}$  in the spacecraft YZ plane rotates with a rate approximately equal to the angular rate of the spacecraft about its X axis. Furthermore, the component of  $\mathbf{h}$  tracks reasonably closely that of  $\mathbf{H}$  in the YZ plane under the 2-axis control. Therefore, it is possible to use the measurable  $\mathbf{h}$  for the estimation of the X angular rate, or the rate about the desired sun-line axis.

Because the rate of change of the angular momentum of a reaction wheel is approximately equal to the net axial torque, which is the applied motor torque minus drag torque, commanded wheel torque\* can also be applied in sun-line rate estimation. The use of  $\mathbf{T}_c$  and  $\mathbf{h}$  together allows the estimation to be done without the need to differentiate any measured data. An example is a quantity  $\mathbf{u}$ , which is roughly equal to the sun-line rate scaled by a non-negative multiplier, defined as

$$\mathbf{u} = (\mathbf{T}_c \times \mathbf{h}) \cdot \mathbf{s}_d$$

\* Alan Reth of NASA GSFC suggested to the authors the use of commanded wheel torque for sun-line rate estimation.

The multiplier is roughly equal to  $h_y^2 + h_z^2$ . A similar idea of using wheel torque and momentum for estimation of the motion about the sun line had been proposed for the International Ultraviolet Explorer if all of its gyros had failed.<sup>3</sup> Figure 9 shows the comparison of  $\mathbf{u}$  and the true sun-line rate with  $\mathbf{u}$  scaled by the inverse of a multiplier. It is clear that  $\mathbf{u}$  in steady state is approximately proportional to the sun-line rate and may be used to augment the 2-axis control.

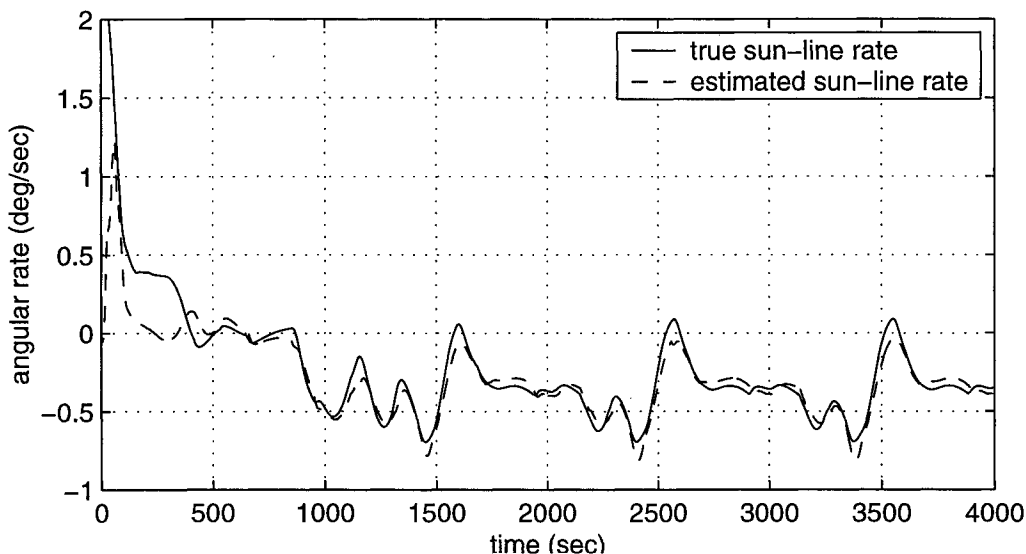


**Figure 9: Estimated Sun-Line Rate Quantity vs. True Sun-Line Rate under 2-Axis Control in Non-ideal Conditions**

### Triana Safehold Control

The control law for Triana Safehold incorporates the rough knowledge of the sun-line rate in the 2-axis controller described above. With this control law the torque command becomes

$$\mathbf{T}_{c1} = \mathbf{I} \left[ k_p \text{Limit} (\theta_e) + k_v \left( \frac{d}{dt} s \right) \times s \right]$$

$$\mathbf{T}_{c2} = \mathbf{I} k_w \mathbf{u} s_d$$

$$\mathbf{u} = (\mathbf{T}_{c1} \times \mathbf{h}) \cdot \mathbf{s}_d$$

$$\mathbf{T}_c = \mathbf{T}_{c1} + \mathbf{T}_{c2}$$

$$\theta_e = \mathbf{s} \times \mathbf{s}_d$$

$$\mathbf{T}_{wc} = \mathbf{W}^+ \mathbf{T}_c + \mathbf{T}_{mr} + \mathbf{T}_{dc}$$

where  $k_w$  is a scalar gain applied on  $\mathbf{u}$ . Since the sun-line rate quantity  $\mathbf{u}$  includes in it a non-negative variable scale factor, the value for gain  $k_w$  should be chosen with the scale factor taken into consideration. Furthermore, the fact that  $\mathbf{u}$  is only a good indicator of sun-line rate in steady state means that  $k_w$  should be sufficiently small so that the transient behavior of the 2-axis control is not adversely affected. Simulating exactly the same case as the one with sun angle shown in Figure 3 with the Triana Safehold control law results in sun angle behavior shown in Figure 10. It is quite easily observed that the use of  $\mathbf{u}$  in the control law can improve the steady-state sun angle performance without degrading the transient behavior. More simulation results generated with a high fidelity model of the Triana's control system are presented below.

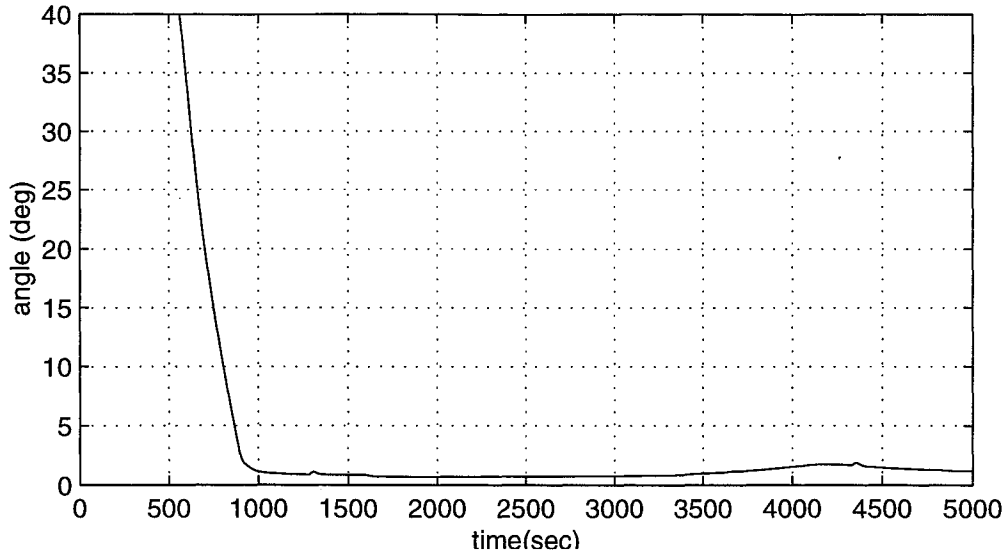


**Figure 10: Sun Angle under Triana Safehold Control with Non-Ideal Condition**

### SYSTEM ANALYSIS

Using the commutation of wheel momentum to estimate the sun-line rate provides Triana with an effective Safehold using the minimum complement of hardware. However, this design also produces a coupled, non-linear system, which cannot be analyzed using the traditional linear stability analysis techniques. As more complex algorithms are implemented, the problem of analyzing a non-linear system is becoming more prevalent. To meet Triana's stability proof requirement, a non-conventional approach has been tried. It is briefly described here to provide the readers some understanding as to what has been done. The analyses address a coupled dynamic system, including both rigid and flexible dynamics.

#### Stability of Periodic Orbits

Similar to what is shown in Figure 7, Triana Safehold control also exhibits a periodic steady-state motion, but with much longer period. Given a system which exhibits a periodic orbit as its steady state, the dynamical behavior will be repeatable from cycle to cycle. If the system is stable, any perturbation away from this periodic steady state, will return to steady-state orbit. Such perturbation is demonstrated in Figure 11. By linearizing the perturbed equations of motion about this steady state, we can examine the system's stability. This linearized perturbed equations have periodic coefficients and can only be obtained from numerical simulation of the non-linear model. The process involves repeated simulation for one period with the initial values of the system states varied by small amounts from their steady state values. The changes in initial values are chosen to be orthogonal from run to run and to span the space of the states. The objective is to evaluate the state transition matrix at the end of one period. The largest magnitude of the eigenvalues of this state transition matrix, except the one corresponding to an eigenvector that is tangent to the orbit, is indicative of system stability for the given perturbation. This numerical solution must be repeated for a great number of perturbations, which would entail hundreds of successive numerical solutions, making this stability proof fairly tedious to complete, especially for a long orbit period. This leads the analysis team to pursue a more streamlined stability proof.

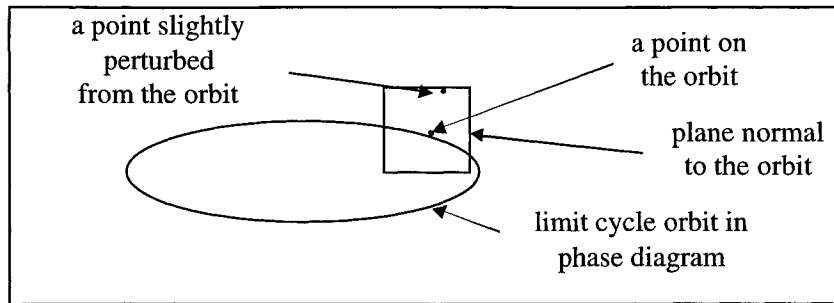


**Figure 11: Perturbation from a Periodic Orbit**

### Stability of Equilibrium

In ideal conditions, a spacecraft under the Triana Safehold control behaves just like the 2-axis controller; it reaches an equilibrium with the desired sun line pointing at the Sun without any body rates. Equations of motion governing the perturbation from this equilibrium can be explicitly formulated and linearized into constant coefficient differential equations. Laplace transformation can thus be applied to the linearized perturbation equations. The resulting frequency domain equations are still a coupled, three-axis system, not amenable to conventional frequency domain stability criteria, such as Bode or Nyquist. However, the real parts of the closed-loop system poles determine the stability of the equilibrium. Examining the poles is much more computationally efficient than solving for the state transition matrix as required for determining stability for periodic orbit described above.

Using the equilibrium for Triana stability study requires some basic assumptions, so we will next consider the validity of these assumptions before proceeding to stability results. The effect of periodic orbit is most significant when the orbit period is very short. Simulation shows our Safehold will exhibit a 'fast' cyclic behavior under several conditions. First, if the sun-line rate is nearly unobservable, which occurs when the system momentum is nearly aligned with the sun vector, a non-nominal condition for Triana. Second, if Safehold is subject to very high system momentum, which is a condition outside the Safehold operating requirements. Finally, if Safehold has very high uncompensated wheel drag, which should not occur since the compensation is based on precise hardware data. For these cases, it is probably not a good idea to assume that equilibrium is the steady state motion. However, all of these cases are highly unlikely for the Triana Safehold, so the equilibrium assumption is reasonable.

To further support the equilibrium assumption, the values of control gains that cause instability have been shown to be about the same for both the non-ideal periodic orbit and ideal equilibrium for a few randomly chosen cases. This implies that analysis with both steady-state motions will result in similar stability margins.

### Stability Margins

The steps taken to establish stability margins are as follows: For a given magnitude of system momentum, let its direction vary to span spherical space. Then, using the linearized perturbed equations around an equilibrium, find minimum damping poles of closed-loop system among all these directions. Vary gains and computation delays individually until the minimum damping poles for a given system momentum magnitude have negative damping. The gains and numbers of delay cycles at the point the closed loop poles change from positive to negative damping (from stable to unstable) are indicative of Safehold's gain and phase margins for that system momentum.

Vary the magnitude of system momentum and repeat these steps over a range of system momentum from zero to 27 Nms, which is twice the required operating range. By doing this it has been found that the Triana Safehold has margins of at least 6 dB in gain and 30 degrees in phase over this entire range, well within our stability requirements. The margin results were validated using the Triana simulation, by increasing the gains by the analytically predicted margins and watching the system become unstable as predicted.

## SIMULATION AND RESULTS

This section delves into the closed-loop modeling for the Safehold control mode and then gives results from the simulation to demonstrate performance. Previous sections have already defined the Safehold control law and a brief description of the sensor and hardware complement. What remains is to define the fidelity by which the sensors,

actuators and their respective data are modeled. The Triana high fidelity (HiFi) simulator represents a closed loop modeling of the onboard systems, the spacecraft's environment and the physical laws that govern them. The HiFi simulator was implemented on a UNIX platform using a commercially available modeling and simulation package called Xmath/Systembuild.

The Safehold control law uses a minimal and simplistic sensor configuration, the Coarse Sun Sensor (CSS), to provide both rate and attitude error signals for control, as described above. There are six CSSs grouped in triads, thus two sets of three CSSs. The triad is arranged so that each individual CSS in the set is orthogonal to the other two and each CSS boresight makes the same angle from the X spacecraft axis. A set is mounted on the +X side (earthward) and the -X side (sunward) of the spacecraft. With this configuration the unit sun vector can be observed in any orientation except when the sun is shining in the blind rings of opposing pairs of CSSs. Because the half-cone angle of a CSS is 85 degrees, the blind ring of an opposing pair of CSSs has a width of 10 degrees. It is thus possible for only one or two of the CSSs to see the sun, and this then produces "jumps" in the CSS data when the sun leaves or enters these regions. Since differentiation of the unit sun vector is required in the control law, this discontinuity may cause undesirable effect on the control performance. If the triads were aligned with the spacecraft axes, one of these regions would be in the neighborhood of the desired sun line. This would have caused a problem in steady state when the desired sun line is nearly aligned with the sun vector.

In the HiFi simulator, each CSS is faithfully modeled as generating a positive voltage signal that represents the cosine of the angle between the CSS boresight and the sun unit vector. The CSS sensor model computes this by taking the dot product between each CSS boresight and the true sun vector. The CSS voltage measurements are then limited to values between zero and a threshold corresponding to the half-cone angle. To this voltage output is added Gaussian noise, with a standard deviation of 0.001. The voltage signals are then sent to the Utility Hub (Uhub) which combines the voltages from each triad, applies the appropriate sign (whether it is from the +X or -X triad) and outputs a representation in counts of the sun unit vector in body coordinates. The sensor processing routine then takes this vector and converts it to a normalized unit vector, which is the sun unit vector in body coordinates.

The control torques calculated with the Safehold control law are sent to the IRWA. The simulator computes realistic torque capacity based on current speed, and maximum voltage and power available, and limits the actual torque delivered to each wheel. The tach measurements are computed from the current wheel momentum and corrupted with a Gaussian noise process depending on the wheel speeds.

The parameter values used in the Safehold performance simulation define a fully deployed spacecraft configuration and a point in the Lissajous orbit. The spacecraft inertia matrix for this configuration is

$$I = \begin{bmatrix} 251.116 & 3.322 & -36.779 \\ 3.322 & 271.04 & 0.707 \\ -36.779 & 0.707 & 217.5 \end{bmatrix} \text{ kg m}^2$$

Important initialization differences for the various cases are illustrated in Table 1.

**Table 1: Defining Initialization Parameters for Safehold Performance Test Cases**

	True Body Rates (rad/sec)	True System Mom. (Nms)	Initial Angle* ( deg )	Cmd Sun Vector
Case 1	X = 0.0 Y = 0.0 Z = 0.0	X = 0.1484 Y = 3.6318 Z = 3.4332	96.7	Cmd X = -1.0 Cmd Y = 0.0 Cmd Z = 0.0
Case 2	X = -0.04872 Y = -0.00271 Z = -0.03942	X = -10.790 Y = -0.9228 Z = -6.784	96.7	Cmd X = -1.0 Cmd Y = 0.0 Cmd Z = 0.0
Case 3	X = 0.0 Y = 0.0 Z = 0.0	X = 2.5981 Y = 0.0 Z = 0.0	71.1	Cmd X = -0.9848077 Cmd Y = 0.1736482 Cmd Z = 0.0
Case 4	X = 0.0 Y = 0.0 Z = 0.0	X = 0.1484 Y = 3.6318 Z = 3.4332	179.85	Cmd X = -1.0 Cmd Y = 0.0 Cmd Z = 0.0

\* Initial Angle is defined as the angle between initial sun vector and desired commanded sun vector.

Triana Safehold control is required to keep the sun pointing to within 15 degrees of the commanded sun vector and acquire the commanded pointing from any point in space within 15 minutes. Once acquired, the Safehold control laws should maintain this pointing indefinitely with minimal ground intervention. Sun angle performance for the four cases are shown in Figure 12.

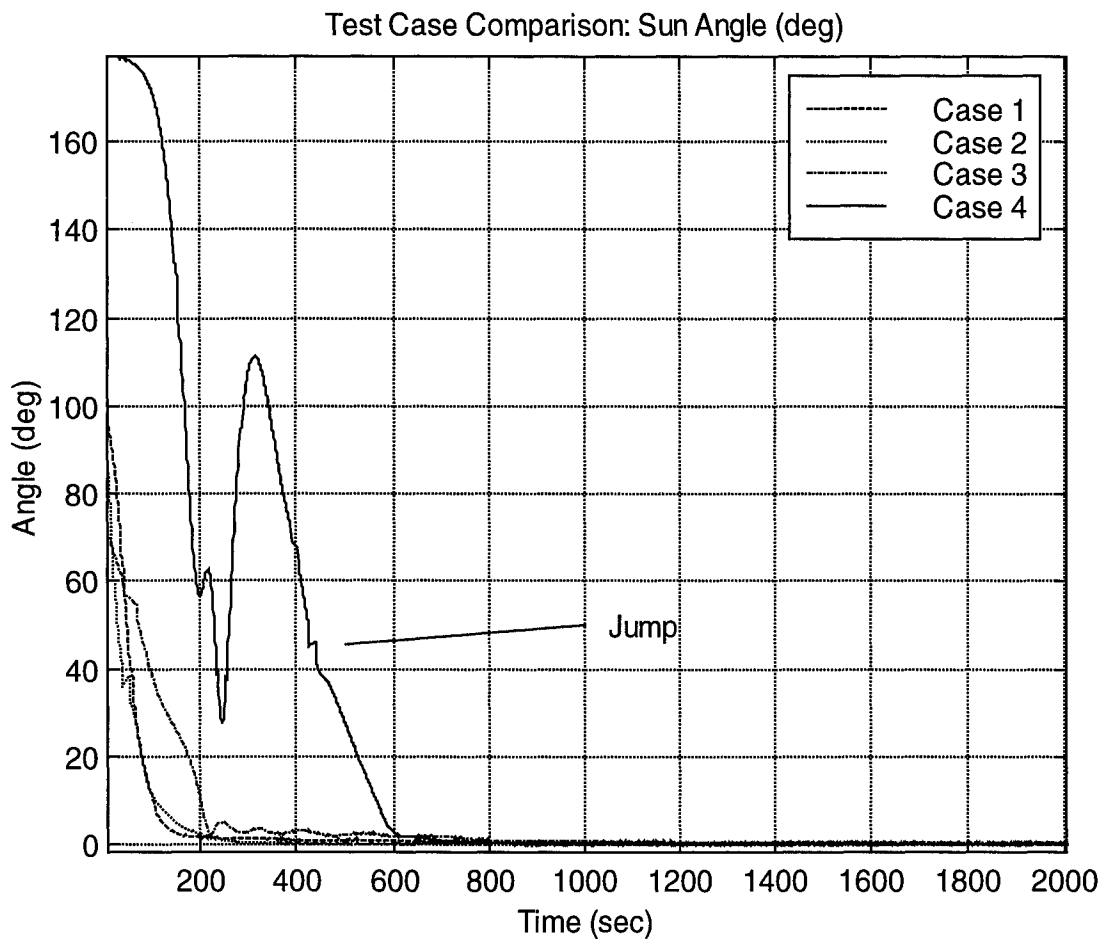


**Figure 12: Sun Angle For Four Cases From HiFi Simulation**

The line marked 'jump' on Case 4 points to an occurrence in which the sun vector is in one of the discontinuous regions where only one or two of the CSS in the triad are active. The sun angle appears to stay constant for a short period of time while the sun vector remains in the region. In fact, the true sun angle continues to change during the period. Figure 13 shows enlargement of the data near zero sun angle for a better assessment of steady-state performance. The small steady-state sun angle is due to the use of sun-line rate estimation in the control law.

## DISCUSSION

Incorporation of a simple, albeit rough, sun-line rate estimation transforms a 2-axis control law into a pseudo 2-and-a-half-axis control law with satisfactory performance. The authors have recognized the potential of further performance improvement if an integral of the estimated sun-line rate quantity is also included in the controller. Cursory simulation supports the idea, but more studies are needed to ensure its validity.

It is also worth mentioning that flexibility in the choice of  $s_d$  exists in the Triana Safehold controller such that an axis other than the nominal sun-pointing axis can be directed toward the sun as demonstrated in case 3 of the simulation results. Although this flexibility is only meant to be used for small pointing offset in Triana operations, it may enable other uses of this control law.

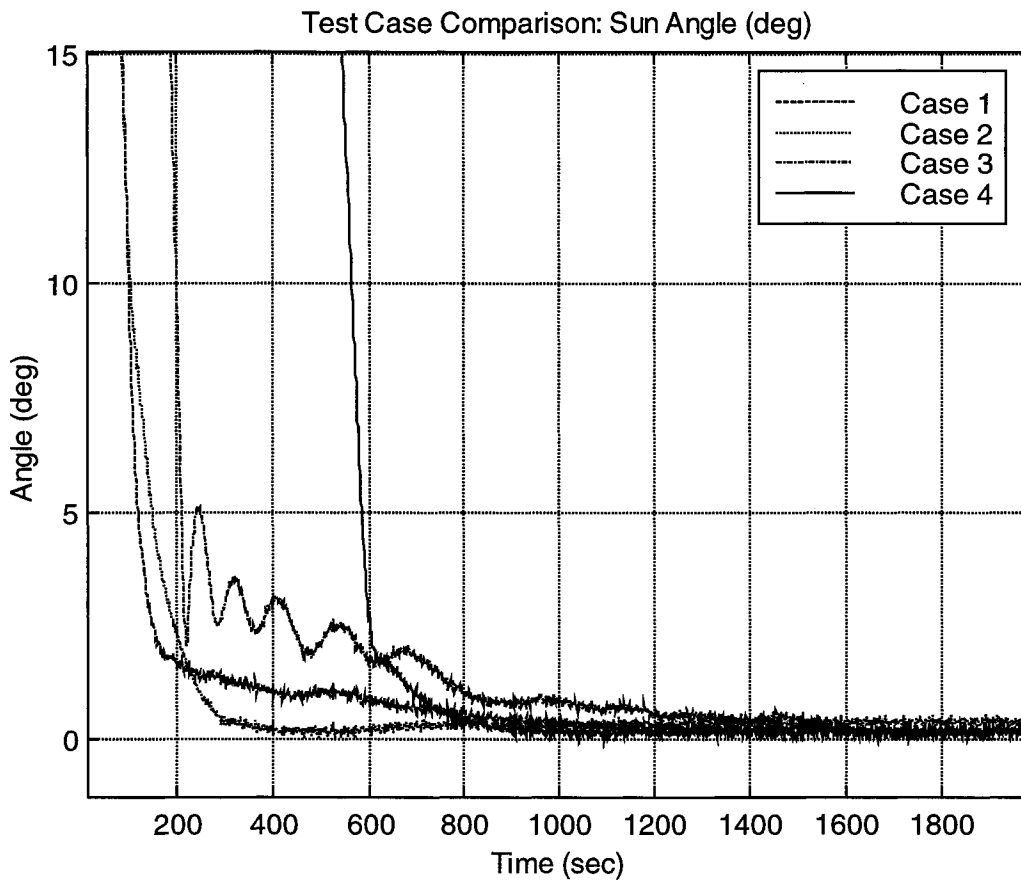


**Figure 13: Steady-State Sun Angle For Four Cases From HiFi Simulation**

**SUMMARY**

Because of Triana’s operational plan, its attitude control system has to function within requirements even when system momentum is near the capacity of its wheel momentum storage. High system momentum, in addition to the worst-case uncompensated wheel drags, puts the gyroless Safehold controller in a particularly difficult situation. Incorporation of a simple, albeit rough, sun-line rate estimation transforms a 2-axis control law into a pseudo 2-and-a-half-axis control law with satisfactory performance. The concept of this estimation originates from observations of the simulation results of a 2-axis control law adapted from previous work. Conservation of system momentum and an expression for system momentum are then used to support the validity of this estimation concept. In addition, a simple algorithm for sun-line rate estimation is introduced and demonstrated to be reasonable in the steady state. Next, the steps taken to establish stability margins for the Triana Safehold control, with sun-line rate incorporated, are described. Results of simulations that includes a high fidelity model of the sun sensors and the wheels are then presented to show performance that satisfy requirements. Finally, suggestions for future improvements and the flexibility of this control law are briefly discussed.

## REFERENCES

1. Andrews, S. F., Campbell, C. E., Ericsson-Jackson, A. J., Markley, F. L. and O'Donnell, J. R., Jr., "MAP Attitude Control System Design and Analysis," Proceedings of the Flight Mechanics Symposium, Goddard Space Flight Center, MD, May 19-21, 1997, pp. 445-454.
2. Hale, J. K. and Kocak, H., Dynamics and Bifurcations, Springer-Verlag, New York, 1991.
3. O'Donnell, J. R., Jr. and Hoffman, H. C., "Zero-gyro Control of the International Ultraviolet Explorer," AIAA Guidance, Navigation and Control conference, Monterey, CA, Aug. 9-11, 1993, Technical Papers Part 1, pp. 530-538.